N. Slavinskaya, J.H. Starcke, M. Abbasi, A. Mirzayeva, U. Riedel, M. Frenklach, A. Packard, W. Li, Wenyu, J. Oreluk, A. Hedge, Consistent Syngas Chemical Mechanism from Collaborative Data Processing. In: Proceedings. 55th AIAA Aerospace Sciences Meeting, 08.-13.01.2017, Paper AIAA 2017-0837, Grapevine, USA.

The AIAA version of the paper is accessible at
http://dx.doi.org/10.2514/6.2017-0837

Consistent Chemical Mechanism from Collaborative Data Processing

N.A. Slavinskaya [1], J.H.Starcke[2], M.Abbasi[3], A.Mirzayeva[4], U.Riedel,[5]
German Aerospace Center (DLR), Institute of Combustion Technology, 70569, Stuttgart, Germany

M. Frenklach [6], A. Packard [7], W. Li[8], J. Oreluk[9], A. Hedge[10]
Mechanical Engineering, University of California at Berkeley, Berkeley, CA 94563, USA

The Bound-to-Bound Data Collaboration (B2B-DC) module of the automated data-centric infrastructure of PrIMe was used for the systematic uncertainty and data consistency analyses of the H_2/CO reaction model (73/17) and 118 experimental targets (ignition delay time and laminar flame speed). The performed consistency analysis of the composed dataset identified a set of experimental data that were inconsistent and therefore removed from the dataset for future investigation. The final consistent dataset with 57 experimental targets and 28 active variables was used for the B2B-DC framework model optimization and analysis on the feasible parameter set. The produced optimized syngas models demonstrated an improved agreement with the studied dataset, as well as with experimental measurements not included in the analysis. The obtained optimized parameter values indicated parameter inadequacy, and the correlation analysis highlighted the direction of possible parameter modifications and model improvement. The initial results demonstrate clear benefits of the PrIMe methods for developing predictive kinetic models.

I. Introduction

To reliably develop predictive reaction models for complex chemical systems requires integration of large amounts of theoretical, computational, and experimental data collected by numerous researchers. The integration entails assessment of the consistency of the data, validation of models, and quantification of uncertainties for model predictions. This approach to the development of mechanistic reaction models consists of conjecturing the reaction mechanism and comparing the predictions of the constructed model to available experimental observations. Typically, such comparisons result in mixed outcomes: some show a reasonably close agreement and some do not. In the latter case, the apparent inconsistency obtained between the model and the experiment is argued to imply either that the model is inadequate or that the experiment (or, rather, its interpretation) is incorrect. The application of computational modeling demands on models to be accurate, reliable, and first of all, predictive.

In the present paper the Data Collaboration module of cyber-infrastructure PrIme[1] (Process Informatics Model) was tested for uncertainty prediction and optimization of chemical reaction model. PrIme[1] is designed for analysis, processing and storage of large amounts of original data using advanced mathematical methods. Here we present preliminary results of the analysis, with a more complete one forthcoming.

Bound-to-Bound Data Collaboration, abbreviated hereafter as B2B-DC, is an optimization-based framework for combining models and experimental data from multiple sources to explore their collective information content. The approach can decisively indicate whether related experimental data are consistent with each other within a specified chemical kinetics model, explore sources of inconsistency, discriminate among differing models, make model interval predictions, and analyze sensitivity of uncertainty propagation. We begin by reiterating some key definitions.[1–8]

[1] Senior research fellow, Chemical Kinetics Department, Nadja.Slavinskaya@dlr.de, AIAA Senior Member.
[2] Senior research fellow, Chemical Kinetics Department, JanHendrik.Starcke@dlr.de.
[3] PhD Student, Chemical Kinetics Department, Mehdi.Abbasi@dlr.de.
[4] PhD Student, Chemical Kinetics Department, Aziza.Mirzayeva@dlr.de
[5] Prof. Head of Chemical Kinetics Department, Uwe.Riedel@dlr.de, AIAA Senior Member
[6] Prof. of University of California, Berkeley, frenklach@berkeley.edu, AIAA Member.
[7] Prof. of University of California, Berkeley, apackard@berkeley.edu.
[8] PhD Student of University of California, Berkeley, wenyuli@berkeley.edu.
[9] PhD Student of University of California, Berkeley, jim.oreluk@berkeley.edu.
[10] PhD Student of University of California, Berkeley, arun.hegde@berkeley.edu.

Quantities of Interest (QoI) is a collection of experimental observations of physical processes, coupled with respective uncertainties, assessed as lower and upper bounds on the observed values, i.e., L_e and U_e for each e-th QoI. This physical process can be represented by a *numerical model*, $M(x)$, with prior knowledge on the domain of parameters, thus constraining each x to an interval $[x_{min}, x_{max}]$ and all together to a hypercube $x \in \mathrm{H}$.

A key requirement for B2B-DC is the formulation of a *dataset* **D** , which entails creation of dataset units for all QoI, e = 1, 2, …, from experimental observations, common kinetic model, and their uncertainties. The computational model $M(x)$ must produce outputs that are consistent with the reported QoI uncertainties.

Hence additional constraints that the true parameters must satisfy are

$$L_e \le M(x) \le U_e \quad \text{for all } e. \tag{1}$$

The subset of $\boldsymbol{H}$ satisfying (1) is called the *feasible set*, $\boldsymbol{\Phi}$, of parameters. $\boldsymbol{\Phi}$ is simply all parameter values that jointly satisfy all of the prior information and are consistent with all model predictions and actual experiment observations. The integral part of the B2B-DC framework is approximation of the $M(x)$ outputs for given QoI by quadratic surrogate models [7], and hence the feasible set, can be define as

$$\Phi := \{x \in \mathrm{H}: L_e \le M_e(x) \le U_e \quad \forall \mathrm{e}\} , \tag{2}$$

where $M_e(x)$ designates a surrogate model of e-th QoI. A parameter value that is not in Φ is at odds with at least one of these constraints.

In this way, the first "bound" in the "bound-to-bound" nomenclature is associated with (a) the form of the prior information, namely that the true model parameters must be both contained in the parameter hypercube H (in the form of bounds on the components), and (b) the true parameters must result in model predictions of all training experiments that are within the measurement bounds declared by the experimenters, namely $L_e \le M_e(x) \le U_e$ for all e. Together, these are the "bounds" that define Φ. The following B2B-DC computations (model parameter analysis and optimization) can be performed only if the feasible set Φ is non-empty. A parameter value that is not in $\boldsymbol{\Phi}$ is at odds with at least one of these constraints.

Dataset consistency is analysis that examines the existence of a feasible parameter vector by determining the consistency measure[2] C_D of dataset **D**,

$$\begin{aligned} C_\mathrm{D} = \max_{\gamma,\, x \in \mathrm{F}} \gamma, \quad & \text{subject to (for all } e\text{):} \\ & (1-\gamma)\frac{L_e - U_e}{2} \le M_e(x) - \frac{U_e + L_e}{2} \\ & M_e(x) - \frac{U_e + L_e}{2} \le (1-\gamma)\frac{U_e - L_e}{2}. \end{aligned} \tag{3}$$

In this definition, the original constraints (1) are augmented with a scalar γ, where positive values of γ imply tightening of the constraint (dataset is consistent) and negative values imply loosening (dataset is inconsistent). The consistency measure, C_D, quantifies how much the constraints can be tightened while still ensuring the existence of a set of parameter values whose associated model predictions match (within the bounds) the experimental QoI.

Model prediction is the prediction interval for property P by model M_P that is consistent with all of the model/observation pairs in the dataset. The B2B-DC computation expresses that into two optimization problems for the lower and upper interval endpoints, L_P and U_P,

$$\begin{aligned} L_\mathrm{P} &:= \min_{x \in \mathrm{F}} M_\mathrm{P}(x) \\ U_\mathrm{P} &:= \max_{x \in \mathrm{F}} M_\mathrm{P}(x) \end{aligned} \tag{3}$$

The length $U_\mathrm{P} - L_\mathrm{P}$ quantifies the amount of uncertainty in M_P's value conditioned on the fact that the true parameter vector is contained in the feasible set $\boldsymbol{\Phi}$.

The results of the proposed analysis suggest a sequential procedure with step-by-step identification of outliers and inspection of the causes. The analysis identifies a specific direction to follow for improving dataset consistency and provides an estimate of the extent of possible improvement. Altogether, this numerical approach offers a tool for assessing experimental observations and model building and improvement.

In the present paper Data Collaboration module of PrIme[1] was applied to the H_2/CO sub-system of the kinetic model[9] to

1) test the numerical algorithms, modules and user interface of the PrIMe;
2) investigate an algorithm of the PrIMe dataset construction;
3) test the different optimization strategies of chemical kinetic model.

The CO/H_2 mixture oxidation chemistry is the principal building block in the hierarchy of hydrocarbon oxidation models. The main part of the most important reactions influencing the combustion of different types of hydrocarbons follows from this reaction sub-system. In recent years, the role of syngas in sustainable combustion processes and promising syngas utilization for power generation triggered further characterization of the CO/H_2 combustion system. As a result, extensive experimental and numerical studies[10] have been performed to investigate the CO/H_2 oxidation mechanism comprehensively.

II. PrIMe DataSet

A. Reaction Model

The H_2/CO sub-model (6 elements, 17 species, 73 reactions) of C_1-C_2 reaction mechanism[9] was used to perform systematic uncertainty and consistency analyses with the Data Collaboration module of PrIme to obtain the feasible set sampling for the base H_2/CO chemistry of DLR reaction data base. The reaction rate coefficients in the examined sub-model were reviewed with further attention to the pressure depending and multichannel reactions. In comparison to the study,[9] the reaction rate coefficients for OH+OH(+M)=H_2O_2(+M) and CO+O(+M)=CO_2(+M) were replaced with values following from.[11–13] The input model together with results of validation can be found online: https://teamsites-extranet.dlr.de/vt/DLR-Mechanism/SitePages/Home.aspx. The uncertainty factors for rate coefficients were assumed equal to the proposed ones in the sources or evaluated from statistical treatment of the different data:

$$f_u(T) = \frac{k_{upper}(T)}{k_0(T)}$$

$$f_l(T) = \frac{k_0(T)}{k_{low}(T)} \quad , \tag{4}$$

where k_0 is the nominal rate coefficient , k_{low} and k_{upper} are lower and upper bounds.

The studied sub-model was extended with OH^* reaction sub-mechanism from[14] to reproduce more precisely the ignition delay times recorded in shock tubes by the OH^* chemiluminescent measurements and was presented in the xml format adopted in PrIMe.[1] A preferred key (or PrIMe ID) was prescribed to each structural element in the reaction scheme. Each structural element has a link with the reference information file. Such constructed set of files defines the reaction model *M(x)* recorded in PrIMe. The model active parameters, i.e., pre-exponential factors of the reaction rate coefficients of the most influential reactions, used for the feasible set construction were identified via sensitivity analysis performed for each QoI. They are reported in Table1.

B. Ignition-delay-time QoI

Quantification of uncertainties in the shock tube is ultimately needed prior to undertaking any tuning of the kinetic parameters to match ignition targets. If some active phenomena in the shock tube experiments cannot be described by assuming homogeneous conditions (constant V, U system) behind the reflected shock, they are classified as “non-idealities” in the shock tube experiments.[22–31] Both, facility-dependent effects and energy-release phenomena can increase the non-idealities and influence the instrument readings, thus adding to the uncertainty of experimental data. For the syngas mixtures, the two regimes of ignition should be recognized: weak ignition - the non-uniform and distributed ignition and strong ignition- initiated by auto ignition at the end wall of the shock-tube and propagating through the mixture.[27]

Although, the non-idealities present in shock tubes have been well-discussed, [22–31] the quantitative evaluation of their effects on the reported ignition delay data is a very crucial problem. To evaluate the uncertainty bounds of the measured observations included in the dataset, the empirical algorithm is proposed. For that, the most strong non-

Table1. Active variables

#	active variables	*A*	*n*	E_a (K)	Ub	Lb	Ref.
(R1)	$H_2+O_2<=>OH+OH$	2.400E+13	0.4700	35121.00	0.1	10	[50]
(R2)	$H+HO_2<=>O_2+H_2$	2.000E+14	0.0000	1030.00	0.50	2.00	[15]*2
(R3)	$H+O_2(+M)<=>HO_2(+M)$	4.660E+12	0.4400	0.00	0.85	1.15	[16]
(R4)	$H + H + M <=> H_2 + M$	7.470E+17	-1.0000	0.00	0.32	3.16	[17]
(R5)	$CO + O_2 <=> CO_2 + O$	1.260E+13	0.0000	23682.94	0.20	5.01	[18]
(R6)	$H + HCO <=> H_2 + CO$	9.000E+13	0.0000	0.00	0.50	2.00	[15]
(R7)	$HCO + O_2 <=> CO + HO_2$	1.350E+10	0.6800	-236.00	0.40	2.50	[15]
(R8)	$CO + HO_2 <=> CO_2 + OH$	1.150E+05	2.2800	8775.00	0.32	3.16	[19]
(R9)	$CO + O (+M) <=> CO_2 (+M)$	1.362E+10	0.0000	1242.0	0.32	3.16	[20]
(R10)	$H+O+M<=>OH +M$	7.730E+18	-1.0000	0.00	0.20	5.01	[18]
(R11)	$H_2+O<=>OH+H$	3.820E+12	0.0000	4000.00	0.63	1.58	[15]
(R12)	$H+HO_2<=>O+H_2O$	1.440E+12	0.0000	0.00	0.32	3.16	[15]
(R13)	$H+H_2O_2<=>OH+H_2O$	1.020E+13	0.0000	1800.58	0.50	2.00	[15]
(R14)	$OH+OH<=>O+H_2O$	3.350E+04	2.4200	-970.00	0.70	1.40	[15]
(R15)	$O+H_2O_2<=>OH+HO_2$	8.430E+11	0.0000	2000.00	0.50	2.00	[15]
(R16)	$H+HO_2<=>OH+OH$	4.000E+14	0.0000	700.00	0.70	1.40	[15]
(R17)	$OH+HO_2<=>O_2+H_2O$	2.890E+13	0.0000	-250.00	0.63	1.60	[15]
(R18)	$O+HO_2<=>OH+O_2$	1.630E+13	0.0000	-224.00	0.32	3.16	[15]
(R19)	$OH+H_2<=>H+H_2O$	2.160E+08	1.5200	1740.00	0.65	1.63	[15]
(R20)	$H+O_2<=>O+OH$	1.900E+14	-0.0970	7560.00	0.80	1.26	[15]
(R21)	$H+H_2O_2<=>HO_2+H_2$	1.690E+12	0.0000	1889.58	0.32	3.16	[15]
(R22)	$OH+H_2O_2<=>HO_2+H_2O$	1.930E+12	0.0000	215.00	0.50	2.00	[15]
(R23)	$HO_2+HO_2<=>O_2+H_2O_2$	1.320E+11	0.0000	-820.30	0.40	2.50	[15]
(R24)	$O+HCO<=>OH+CO$	3.010E+13	0.0000	0.00	0.50	2.00	[15]
(R25)	$O+HCO<=>H+CO_2$	3.010E+13	0.0000	0.00	0.50	2.00	[15]
R(26)	$CO+OH<=>CO_2+H$	1.010E+13	0.0000	8050.00	0.80	1.26	[15]
R(27)	$HCO+O_2<=>OH+CO_2$	1.350E+10	0.6800	-236.00	0.40	2.50	[15]
R(28)	$HCO+M<=>CO+H+M$	4.750E+11	0.6600	7485.00	0.50	2.00	[21]

ideality phenomena[22–31] were determined across the investigations and the facility-related and fuel-related factors, which affect these phenomena, have been identified.

The dominant non-ideality phenomena were attributed to two gas dynamics effects: i) boundary layer formation after incident shock wave interacts with reflected shock-wave (resulting in inhomogeneities of *T* and *p* behind the shock-wave and shock bifurcations); ii) post-shock compression (interaction of the reflected shock-wave with the contact surface). The second most important phenomena influencing the measurements uncertainty is energy-release: the weak regime (the non-uniform/distributed ignition) and the strong regime (initiated by auto ignition at the end wall of the shock-tube) of ignition. The factors which influence these phenomena are: operating conditions; driven section length; driven section diameter; measurement duration; mixture dilution and nature of Carrier Gas (CG).

In the first column of the Table 2, factors, which influence the shock tube measurement error, are summarized. In the second column operating conditions which influence these factors are indicated. The possible errors, caused by these factors and the parameter change, leading to possible error increase, are evaluated in the third column.

It was found that experimental data obtained by using large diameter shock tubes (~ 10cm), dilute fuel/oxidizer mixtures in monoatomic gases, and short test times (less than about 500 μs) have the lowest uncertainty level. A correspondence with the diameter of the shock-tube and weak ignition is found: the larger diameter leading to an ignition delay close to that of a homogeneous reactor.

Table 2.Experimental Ignition Delay Data: uncertainty factors

Facility-related and fuel-related factors affecting the non-ideality phenomena and uncertainty in shock tube measurements	**Operating conditions influencing the factors**	**Contribution in uncertainty correlated with Operating conditions**
Weak and strong ignition (fuel)	T, p, ϕ, CG,	Low T, p, ϕ>0.3 ~ 10 times
Non-ideal gas dynamics behind the reflected shock wave (T, p non-uniformities)	T, p, t_{meas}, CG,	27%-17% Small Dilution ↓
Post-shock compression	T, p, t_{meas}, CG,	dP/dT ≈ 2-6% /ms dT/dt ≈ 1.2%/ms
Radical impurities	T, p, CG, Person	dilution↑, T,p ↓ ; **?**
Temperature measurements	Measurement location	5%
Pressure measurements	T, Measurement location	10%
Concentration measurements (the steepest rate of change)	T, Measurement location	5%

Table 3. Ignition delay time measurements selected model validation.

***P*, MPa**	**Composition**	φ	T_5**, K**	**Ref.**
0.061-1.82	20%CO/ 80%H_2 40%CO/ 60%H_2 80%CO/ 20%H_2 90%CO/ 10%H_2	0.5	890-1285	Kalitan et al.[32]
1.11-3.24	CO/ H_2/CO_2/O_2/N_2	0.5	630-1150	Petersen et al.[33]
0.12-0.14	80%CO/ 20%H_2 90%CO/ 10%H_2	0.5 and 1.0	909-965	Mertens et al.[34]
1.41-1.72	50%CO/ 50%H_2 95%CO/ 5%H_2 Dilution 1: 2, 5, 10	0.5 – 1.0	1048-1259	Herzler et al.[35]
0.1; 0.61; 1.21; 3.24	50%CO/ 50%H_2 90%CO/ 510%H_2 Dilution 98% Ar	0.5	980-2004	Krejci et al.[36]

It was assumed, that in the best case (strong ignition, diluted mixture, t_{meas} = 50ms – 500ms, shock tube diameter > 10 cm, length of driven-section > 8m) the uncertainty can be assumed ~15%. Deviations from these conditions are evaluated by adding a 5% uncertainty for each criterion not satisfied to the ideal case. For measured

ignition delay time longer as 1000 μs 5% uncertainty is added per every 1000 μs. Radical impurities were evaluated as extra 5% uncertainty to the ideal case.

Table 4. Ignition delay QoI selected for the analysis.

Ref.	Driven section length, m	Internal diameter, cm	Temperature interval, K	Pressure, MPa	φ	Dilution	$t_{meas,}$ μs	Integrated uncertainty %
Kalitan et al.[32]	10.7	16.2	< 1000 **+5%**	<1.5	0.5	none **+5%**	100-500	***30***
Kalitan et al.[32]	10.7	16.2	< 1000 +5%	<1.5	0.5	none +5%	500-1000 +5%	***35***
Kalitan et al.[32]	10.7	16.2	< 1000 +5%	<1.5	0.5	none +5%	1000-2000 +10%	***40***
Kalitan et al.[32]	10.7	16.2	> 1000	<1.5	0.5	none +5%	100-600 +5%	***30***
Petersen et al.[33]	10.7	16.2	< 1000 +5%	>1.5 +5%	0.5	none +5%	500-1000 +5%	***40***
Petersen et al.[33]	10.7	16.2	< 1000 +5%	>1.5 +5%	0.5	none +5%	1000-2000 +10%	***45***
Petersen et al.[33]	10.7	16.2	< 1000 +5%	>1.5 +5%	0.5	none +5%	2000-3000 +15%	***50***
Mertens et al.[34]	10.7	16.2	< 1000 +5%	<1.5	0.5-1	none +5%	600-2000 +10%	***40***
Mertens et al.[34]	10.7	16.2	< 1000 +5%	<1.5	0.5-1	yes	600-1200 +10%	***35***
Herzler et al.[35]	11.12	9.82	> 1000	>1.5 +5%	0.5	yes	300-500	***25***
Herzler et al.[35]	11.12	9.82	> 1000	>1.5 +5%	0.5	yes	500-1000 +5%	***30***
Herzler et al.[35]	11.12	9.82	> 1000	>1.5 +5%	0.5	yes	500-1000 +5%	***30***
Kéromnès et al.[36]	4 .72 +5%	15.24	> 1000	<1.5	0.5;1	yes	20 -500	***25***
Kéromnès et al.[36]	4 .72 +5%	15.24	> 1000	<1.5	0.5;1	yes	500 -1000 +5%	***30***
Kéromnès et al.[36]	4 .72 +5%	15.24	> 1000	>1.5 +5%	0.5;1	yes	20-500	***30***
Kéromnès et al.[36]	4 .72 +5%	15.24	> 1000	>1.5 +5%	0.5;1	yes	500-1000 +5%	***35***
Kéromnès et al.[36]	4 .72 +5%	15.24	> 1000	>1.5 +5%	0.5;1	yes	1000-2000 +10%	***40***

In Table 3 the shock tube experiments [32-36] used for model validation are collected. On this step of the methodology testing, we selected 95 ignition delay targets for the analysis. The results of uncertainty evaluation obtained with the proposed empirical rule for the syngas ignition delay time experimental values [32-36] to be included in the PrIMe dataset, are collected in Table 4.

Table 5. Evaluation of uncertainty intervals for laminar flame experimental data selected for QoI

φ	***p, MPa***	***Error***	***p, MPa***	***Error***	***p, MPa***	***Error***
0.5-2	0.1÷0.51	10%	0.51÷1.01	15%	>1.01	20%
2.0÷3.0	0.1÷0.51	15%	0.51÷1.01	20%	>1.01	25%
>3.0	0.1÷0.51	20%	0.51÷1.01	25%	>1.01	30%

C. Laminar-flame-velocity QoI

Syngas flame velocities at 0.1-0.5 MPa have been investigated by using almost all known techniques.[37-40] The flame velocity data at high pressures are relatively sparse. Experimentalists consider the current uncertainties of laminar flame speed measurements to be in a range of about 5–10%, but also indicating its increase with pressure (>0.5 MPa) and fuel-air ratio (φ>2).[37-40]

Uncertainty bounds of experimental data were evaluated from studies[37-40] and analysis of the current syngas atmospheric laminar flame speed data distribution, which can be found in[41] From the data analysis following from[37-44], the uncertainty of available data can be assumed to be 10% for φ< 2, 15% for 2 < φ< 3, and 20% for φ>3.

Table 6. Laminar flame speed measurements selected for model validation

#	***Ref.***	***Mixture***	***p, MPa***	***Prime ID***	***To***, K	φ	***Error***
1	Sun et al.[19]	50/50% CO/H_2/air	0.1	a00000128	300	0.8	10%
2	Sun et al.[19]	50/50% CO/H_2/air	0.1	a00000129	300	1.2	10%
3	Sun et al.[19]	50/50% CO/H_2/air	0.1	a00000130	300	2.5	15%
4	Sun et al.[19]	95/5% CO/H_2/He	0.5	a00000249	300	2	15%
5	Sun et al.[19]	95/5% CO/H_2/He	1.0	a00000250	300	0.75	15%
6	Sun et al.[19]	95/5% CO/H_2/He	1.0	a00000252	300	1.4	15%
7	Sun et al.[19]	95/5% CO/H_2/He	2.0	a00000253	300	1	20%
8	Sun et al.[19]	95/5% CO/H_2/He	4.0	a00000257	300	1.4	20%
9	Sun et al.[19]	50/50% CO/H_2/He	0.5	a00000124	300	3.5	25%
10	Sun et al.[19]	50/50% CO/H_2/He	1.0	a00000125	300	1	15%
11	Sun et al.[19]	50/50% CO/H_2/He	1.0	a00000126	300	1.8	15%
12	Sun et al.[19]	50/50% CO/H_2/He	1.0	a00000127	300	3.5	20%
13	Natarajan et al.[42]	50/50% CO/H_2/air	0.1	a00000282	700	0.73	10%
14	Natarajan et al.[42]	50/50% CO/H_2/air	0.1	a00000280	700	0.9	10%
15	Sun et al.[19]	95/5% CO/H_2/air	0.1	a00000260	300	1	10%
16	Sun et al.[19]	95/5% CO/H_2/air	0.1	a00000261	300	1.5	10%
17	Hassan et al.[43]	95/5% CO/H_2/air	0.05	a00000269	300	1	10%
18	Hassan et al.[43]	95/5% CO/H_2/air	0.1	a00000271	300	0.6	10%
19	Sun et al.[19]	95/5% CO/H_2/He	2.0	x00000460	300	1.6	20%
20	Sun et al.[19]	95/5% CO/H_2/He	2.0	x00000460	300	3	25%
21	Sun et al.[19]	95/5% CO/H_2/He	4.0	x00000461	300	2	25%
22	Natarajan et al.[44]	50/50% CO/H_2/He	1.5	x00000471	600	0.6	20%
23	Natarajan et al.[44]	50/50% CO/H_2/He	1.5	x00000471	600	0.6	20%

The uncertainties for experimental data measured at higher pressure have been evaluated by adding 5%. The empirical rule applied for uncertainties evaluation of laminar speed data can be found in Table 5.

The 23 laminar flame speed data included in the dataset are taken from studies[19, 42-44], Table 6. They are selected to cover as optimal as possible the full range of operating conditions available in the literature.

A preferred key (or PrIMe ID) was prescribed to each experimental target. In this way, each structural element has a "pointer" to the referenced information and/or file. All the experimental data were documented in the PrIMe Data Warehouse.[1] Selected for analysis experimental QoI are described in the dataAttribute files of the PrIMe data collection.[1] These QoI together with the corresponding model $M_e(x)$ and the experimental and parameter bounds form a dataset. The complete model and experimental data are available in the PrIMe Data Warehouse.[1]

III. General Results

The ignition delay times and laminar flame speeds were modeled with numerical tools of PrIMe,[1] numerical packages CHEMKIN II[45] and Chemical Workbench.[46] The ignition delay time was computationally defined by the peak in the OH or OH* concentration, temperature, or pressure. It is pointed in the attribute files of PrIMe Warehouse. The thermal diffusion model was applied for calculation of one-dimensional freely propagating laminar premixed flame using CHEMKIN II with over 1000 grid points for each condition.

A. Dataset Consistency (Data Quality)

The consistency analysis was performed for the dataset that included first 95 QoI of ignition delay times, 23 QoI of laminar flame speed and 28 active parameters (Tables 1, 5, and 6). Initially, before performing the consistency test, 12 experimental QoI were excluded from the dataset because the ignition delay times could not be reproduced at all: the calculated OH* profile in these cases did not exhibit a maximum. All other 83 ignition delay targets were fitted with quadratic surrogate models with on-design errors not exciding 1% and off-design errors below or about 2%. The initial results of the consistency analysis indicated a high degree of inconsistency of ignition delay QoI. To bring the dataset to consistency, QoI bounds were changed, as shown in Fig. 1 and in details in Table 6.

The further consistency analysis performed for 83 ignition delay targets and 23 laminar flame speeds determined that ignition-delay QoI with large bound changes, Table 6, and eight computed flame QoI values (flames F2, F4, F13-17, F22 in Table 5) fell outside their respective uncertainty bounds, should be assumed as self-inconsistent data and hence were excluded from the dataset. Self-inconsistency means that no point in the rate constant domain $\boldsymbol{H}$ can reproduce the experimental QoI within its uncertainty bounds.

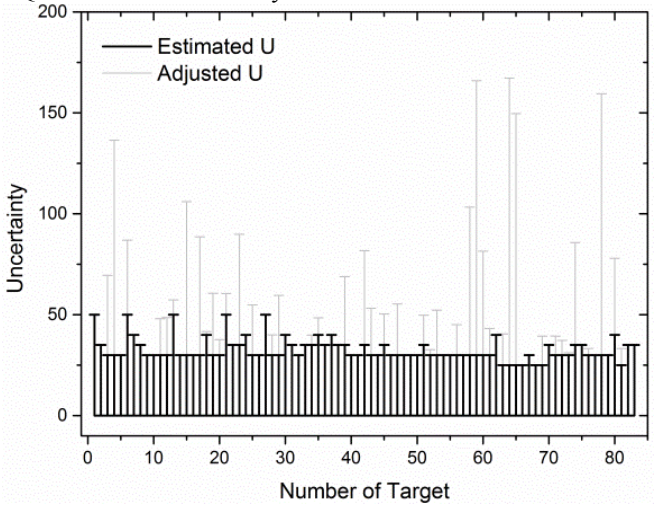

Figure 1. The bound change in ignition delay QoI obtained by data consistency analysis.

Table 6. Results of B2B-DC analysis for ignition delay time targets (Low T: T<1000K High p:p > 1 MPa). Blue color: targets excluded since calculated profile did not exhibit maximum OH*. Gray color: targets excluded due large UQ

#	T_5, K	p_5, MPa	Prime ID	Current Uncertainty,%	Minimum UQ, %	Refs.	Comment
1	916	0.11	a00000179	**50**		**25**	
2	954	0.12	a00000181	**35**		**25**	
3	993	0.10	a00000183	**30**	**69,4476**	**25**	**Low T**
4	1074	0.11	a00000186	**30**	**136,4403**	**25**	
5	1151	0.1	a00000188	**30**		**25**	
6	914	0.11	a00000105	**50**	**86,922**	**25**	**Low T**
7	951	0.11	a00000131	**40**		**25**	
8	996	0.11	a00000132	**35**		**25**	
9	1072	0.11	a00000133	**30**		**25**	
10	1175	0.1	a00000135	**30**		**25**	
11	1187	0.1	a00000136	**30**	**47,986**	**25**	
12	1241	0.1	a00000107	**30**	**48,6134**	**25**	
13	900	0.06	a00000110	**50**	**57,3177**	**25**	**Low T**
14	1026	0.11	a00000111	**30**		**25**	
15	1162	0.1	a00000112	**30**	**105,9988**	**25**	**High P**
16	936	0.12	a00000113	**40**		**25**	
17	**1015**	**0.11**	a00000189	**30**		**25**	
18	1183	0.11	a00000190	**30**	**88,6136**	**25**	
19	929	0.26	a00000191	**50**		**25**	
20	992	0.26	a00000192	**40**	**41,6159**	**25**	
21	1058	0.26	a00000114	**30**	**60,6507**	**25**	
22	1063	0.31	a00000193	**30**	**37,6735**	**25**	
23	1015	1.39	a00000213	**50**	**60,4698**	**25**	**High P**
24	1114	1.51	a00000194	**35**		**25**	
25	1190	1.70	a00000115	**35**	**89,866**	**25**	**High P**
26	960	0.12	a00000116	**40**		**25**	
27	1052	0.11	a00000195	**30**	**54,8933**	**25**	
28	1197	0.11	a00000196	**30**		**25**	
29	981	0.27	a00000197	**50**		**25**	
30	1048	0.25	a00000198	**30**	**40,0207**	**25**	
31	1118	0.25	a00000117	**30**	**59,5535**	**25**	
32	1063	1.45	a00000199	**40**		**25**	
33	1126	1.20	a00000200	**35**		**25**	
34	1265	1.73	a00000118	**30**	**30,0166**	**25**	

35	968	0.12	a00000307	40		25	
36	1033	2.40	a00000317	35		26	
37	1148	2.17	a00000318	35	39,9265	26	High P
38	909	0.119	a00000322	40		27	
39	933	0.116	a00000323	40	48,481	27	Low T
40	947	0.121	a00000324	35		27	
41	932	0.14	a00000223	40		27	
42	956	0.14	a00000224	35		27	
43	965	0.15	a00000225	35	68,8672	27	Low T
44	1046	1.70	a00000226	30		28	
45	1072	1.60	a00000227	30		28	
46	1132	1.64	a00000228	35	81,7297	28	High P
47	1107	1.64	a00000229	30	53,2523	28	High P
48	1159	1.64	a00000230	30		28	
49	1206	1.66	a00000231	35	50,3792	28	High P
50	1165	1.63	a00000232	30		28	
51	1207	1.66	a00000233	30	55,3106	28	High P
52	1259	1.61	a00000234	30		28	
53	1019	1.43	a00000235	30		28	
54	1051	1.55	a00000236	30		28	
55	1097	1.58	a00000237	35	49,7875	28	High P
56	1048	1.62	a00000238	30	32,7013	28	
57	1086	1.57	a00000239	30	52,2544	28	High P
58	1128	1.57	a00000240	30		28	
59	1054	1.58	a00000241	30		28	
60	1090	1.60	a00000242	30	45,0207	28	High P
61	1140	1.61	a00000243	30		28	
62	1057	0.11	a00000308	30	103,2932	25	
63	1263	0.11	a00000309	30	165,9728	25	
64	977	0.23	a00000310	40		25	
65	1149	0.20	a00000311	30	81,5249	25	
66	1304	0.17	a00000312	30	43,152	25	
67	1110	1.29	a00000313	40		25	
68	943	2.26	a00000316	35		26	
69	1299	1.22	a00000334	25	40,4547	29	
70	1182	1.22	a00000335	25	167,1738	29	
71	1096	1.22	a00000336	30		29	
72	1383	1.22	a00000337	25	149,6117	29	

73	1235	1.22	a00000338	**25**		**29**	
74	1099	1.22	a00000339	**30**		**29**	
75	1387	1.22	a00000340	**25**		**29**	
76	1228	1.22	a00000341	**25**	**39,3955**	**29**	
77	1116	1.22	a00000342	**35**		**29**	
78	1264	3.24	a00000343	**30**	**39,4483**	**29**	
79	1243	3.24	a00000344	**30**	**37,2183**	**29**	
80	1185	3.24	a00000345	**35**		**29**	
81	1325	3.24	a00000346	**30**	**31,1241**	**29**	
82	1204	3.24	a00000347	**35**	**85,7406**	**29**	
83	1179	3.24	a00000348	**35**		**29**	
84	1327	3.24	a00000349	**30**	**33,3077**	**29**	
85	1259	3.24	a00000350	**30**		**29**	
86	1166	3.24	a00000351	**40**		**29**	
87	1695	0.16	a00000352	**30**	**159,4249**	**29**	
88	1351	0.16	a00000353	**30**		**29**	
89	980	0.16	a00000354	**40**	**77,9251**	**29**	**Low T**
90	2004	0.16	a00000355	**25**		**29**	
91	1273	0.16	a00000356	**25**	**33,2412**	**29**	
92	992	0.16	a00000357	**35**		**29**	
93	1975	0.16	a00000358	**25**		**29**	
94	1436	0.16	a00000359	**25**		**29**	
95	1027	0.16	a00000360	**35**		**29**	

The 28 active parameters in studied dataset were kept the same as in the original model. Their bounds were not changes as they showed lower sensitivities than those of the experimental QoI uncertainties and also with the aim to have the smallest parameter modifications of the respective literature recommendations. The final dataset for feasible set construction had 57 experimental QoI and 28 active variables.

B. Feasible set construction

While $\boldsymbol{H}$ designates prior information, feasible set $\boldsymbol{\Phi}$ summarizes *posterior* information: all parameter value combinations that satisfy their own bounds and also the QoI included in the dataset bounds. The size and shape of $\boldsymbol{\Phi}$ compared to those of $\boldsymbol{H}$ represent information gained as a result of the B2B-DC analysis. Projection of $\boldsymbol{\Phi}$ on each of the x's yields the posterior range of the parameter uncertainty.[3] For the rest of the parameters, the posterior ranges were the same as the prior ones, indicating that the experimental data included in the present analysis did not aid in narrowing down the uncertainty ranges of these parameters *individually*. However, such an outcome does not necessarily imply no information gain for a given parameter: while the extreme parameter values (bounds) may not change, the feasible set may, and usually does, eliminates some combinations of these parameters with others, which is addressed next.

C. Parameter optimization

While the primary focus of the B2B-DC framework is on prediction over the feasible set, it also supports parameter optimization.[47] Three sets of optimized model parameters were investigated and inter-compared in the present study. The first approach is LS-H, a (weighted) least-squared fit constraining parameter values to their initially assessed uncertainty ranges, $\boldsymbol{H}$. B2B-DC supports two more refined methods of optimization,[47] LS-F and 1N-F, where the objective is minimized with x's being constrained to the feasible set $\boldsymbol{\Phi}$. The three problems are easily expressed as mathematical optimizations. The LS methods minimize the familiar sum of weighted least-squared deviations between the surrogate model prediction and the reported measured value, y_e. The difference lies in where the search takes place: LS-H considers all of H while LS-F restricts the search to F,

$$\text{LS-H}: \quad \min_{x\in \mathrm{H}} \sum_e w_e \left[M_e(x) - y_e \right]^2$$

$$\text{LS-F}: \quad \min_{x\in \mathrm{F}} \sum_e w_e \left[M_e(x) - y_e \right]^2$$

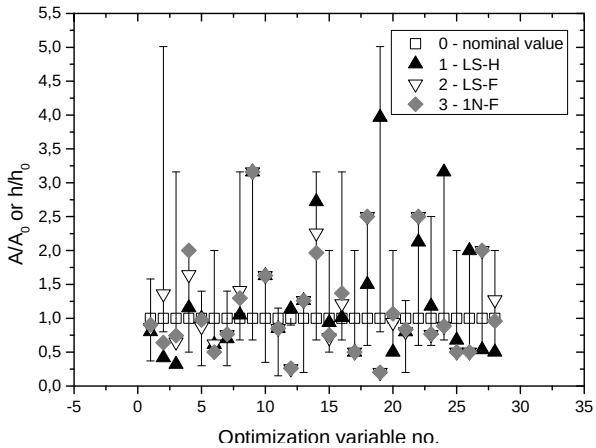

Figure 2. Ratios of optimal to initial values for 28 pre-exponential factors of rate coefficients obtained with methods LS-H, LS-F and 1N-F. Error bars indicate the specified variable ranges.

By contrast, the 1N-F problem treats the nominal parameter vector, the starting set of parameter values ($x_0 = 0$), as "preferred". As we have shown in previsions sections, this parameter set lies outside the feasible region $\boldsymbol{\Phi}$. The goal of the 1N-F method is to find with least number of changes to x_0 a parameter vector that is feasible. Mathematically, the one-norm is a well-known approximation to enforce such sparsity, i.e.,

$$\text{1N-F}: \quad \min_{x\in \mathrm{F}} \left\| x - x_0 \right\|_1$$

The LS-F and 1N-F optimizations were performed with the final dataset, as the two methods are designed to work with an existing feasible set. The ratios of optimized to initial values for 28 rate coefficients obtained with methods LS-F and 1N-F are shown in Fig. 2

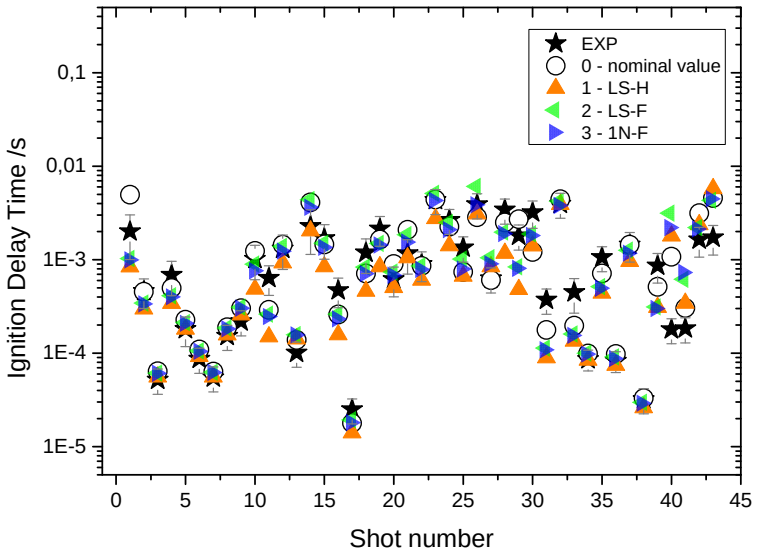

Figure 3. Optimal model predictions of ignition delay times using optimization methods LS-H, LS-F and 1N-F. Nominal value – modeling with original model.

Inspection of the results highlights several features. All optimization methods result in parameter sets that produce a better agreement with experiment than the original model, composed of literature recommendations. The LS-H optimization, constrained only to the prior uncertainty ranges of parameters, results in the lowest average deviation, as expected, but at the expense of violating uncertainty bounds of 13 experimental QoI.

The average deviation produced by LS-F is larger but not significantly than that of LS-H. The 1N-F method gives a larger average deviation, yet it changes the least number of variables. The LS-F and 1N-F optimization methods, with additional constraints to the QoI uncertainties, do not violate

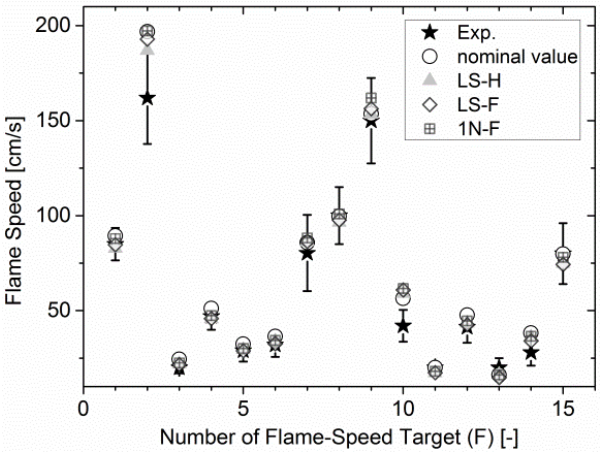

Figure 4. Optimal model predictions of laminar flame speed using optimization methods LS-H, LS-F and 1N-F. Nominal value – modeling with original model.

any of the QoI bounds by design unlike to the LS-H. That demonstrates the main difference between two approaches: LS-H optimization can be identified rater as a fitting, Fig. 3 and 4.

The better agreement of the optimized model with the selected experimental data should not be presumed, however, to be the final step of the analysis. While the obtained optimized parameter values can serve as an indicator for parameter inadequacy, the direction of possible parameter modifications can be further revealed from analysis of correlations. Such correlations are displayed in Figures 5 and 6, which display results of random sampling of the feasible set. Figure 5 depicts correlation plots of selected model parameters. The displayed results illustrate trends in parameter distributions and correlations between different reaction rate coefficients. Figure 6 presents similar information but includes also correlations among QoI and correlations among model parameters and QoI. These diagrams highlight the "bound-to-bound" concept and demonstrate the influence of experimental data on the active parameter distributions. Noteworthy is the fact that the feasible-set regions, identified by the sampled points marked in blue, are not centered for some QoI and for some parameters. If the prior information were exactly correct, both the experiment and the model, than we should have the feasible set centered at the nominal values of parameters and measured QoI, i.e., located in the center of each diagram. The fact that in many cases the feasible set is "pushed" to the boundaries indicates the presence of either systematic errors in experiments or bias in the model. The information provided in the analysis thus helps to focus on the issues (experiments, parameters, model) that need immediate attention in moving toward a more predictive model.

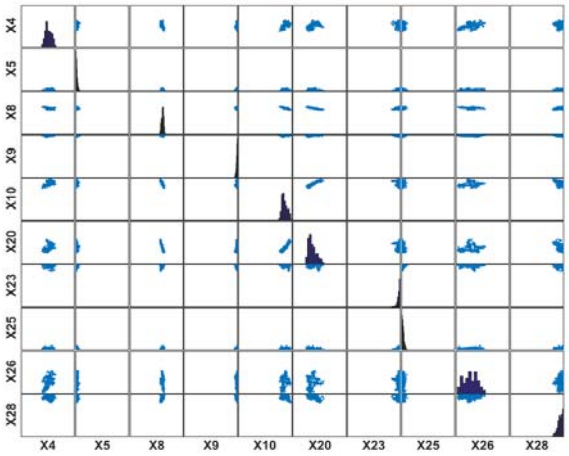

Figure 5. Correlation plots of selected parameters (Table 1). The axis intervals represent their uncertainty ranges, [-1, 1].

Finally, the comparison of model predictions obtained with the original and optimized mechanisms for the experimental QoI is shown in Fig.7. As can be seen in Fig.7, the model optimized on the feasible set improves the experimental reproduction not only for QoI of the dataset but also for those not included in the B2B-DC analysis, Fig.7b. This is in contrast to the results obtained with the model optimized on the entire hypercube H, which does not describe correctly neither the trend nor the values of the experimental observations. This demonstrates the benefits of optimization methods LS-F and 1N-F and generally of the B2B-DC methodology in comparison to the "conventional" optimization, LS-H.

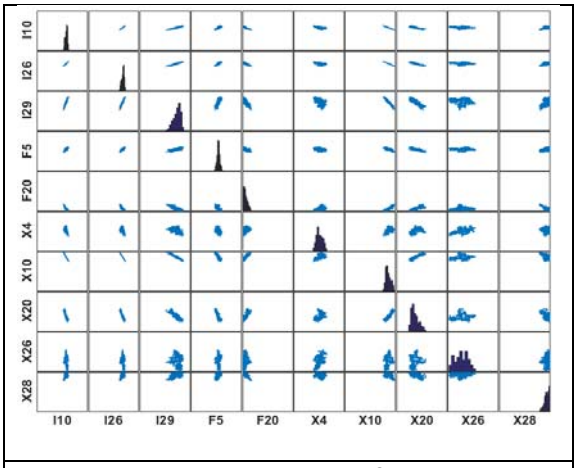

Figure 6. Correlation plots of selected active parameters (X) and of selected ignition-delay (I) and flame-speed (F) QoIs. The QoI axis intervals represent their respective uncertainty ranges, [Le, Ue].

IV. Conclusions

An optimization-based framework B2B-DC of an automated data-centric infrastructure, Process Informatics Model (PrIMe) was applied to the syngas reaction mechanism analysis with the aim to test the PrIMe software facilities. For this purpose, a dataset was constructed based on pertinent experimental observations, chemical-kinetics model, and the associated uncertainties. The 118 experimental Quantities of Interest (QoI) were selected through evaluation of ignition delay time and laminar flame speed uncertainties. The composed dataset was subjected to consistency analysis. One outcome of the analysis was identification of a set of experimental QoI that were most difficult or impossible to match with the model; they were removed from the dataset for future investigation. The final consistent dataset with 57 experimental QoI and 28 active variables was used for model optimization on the feasible parameter set. The optimized syngas models produced with B2B-DC framework demonstrated an improved agreement with the dataset QoI, as well as with experimental measurements not included in the analysis. The obtained optimized parameter values indicated parameter inadequacy, and the correlation analysis highlighted the direction of possible parameter modifications and model improvement. The algorithm of an application of the PrIme Data Collaboration module must be investigated further.

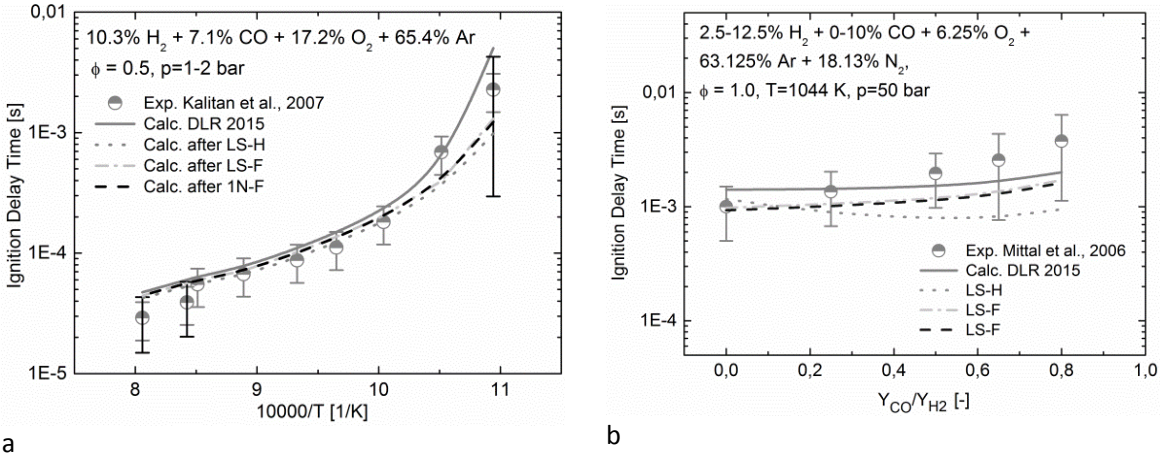

a b

Figure 7. Optimal model predictions of ignition delay times using optimization methods LS-H, LS-F and 1N-F. The bars indicate the specified data and changed ranges. a) experimental data[32] included in the dataset; b) experimental data[48] not included in the dataset.

Acknowledgments

The work at UC Berkeley was supported by the U.S. Department of Energy, National Nuclear Security Administration, under Award Number DE-NA0002375.

References

[1]Frenklach, M., "PrIMe," URL: http://primekinetics.org.

[2]Feeley, R., Seiler, P., Packard, A., and Frenklach, M., "Consistency of a Reaction Dataset," *The Journal of Physical Chemistry A*, Vol. 108, No. 44, 2004, pp. 9573–9583.

[3]Frenklach, M., Packard, A., Seiler, P., and Feeley, R., "Collaborative Data Processing in Developing Predictive Models of Complex Reaction Systems," *International Journal of Chemical Kinetics*, Vol. 36, No. 1, 2004, pp. 57–66.

[4]Russi, T., Packard, A., Feeley, R., and Frenklach, M., "Sensitivity Analysis of Uncertainty in Model Prediction," *The journal of physical chemistry. A*, Vol. 112, No. 12, 2008, pp. 2579–2588.

[5]Russi, T., Packard, A., and Frenklach, M., "Uncertainty Quantification: Making Predictions of Complex Reaction Systems Reliable," *Chemical Physics Letters*, Vol. 499, 1-3, 2010, pp. 1–8.

[6]Frenklach, M., Packard, A., and Feeley, R., "Optimization of Reaction Models with Solution Mapping," *Modeling of Chemical Reactions*, edited by R. W. Carr, 1st ed., Elsevier, Amsterdam, 2007, pp. 243-293.

[7]Seiler, P., Frenklach, M., Packard, A., and Feeley, R., "Numerical Approaches for Collaborative Data Processing," *Optimization and Engineering*, Vol. 7, No. 4, 2006, pp. 459–478.

[8]Frenklach, M., "Transforming Data into Knowledge—Process Informatics for Combustion Chemistry," *Proceedings of the Combustion Institute*, Vol. 31, No. 1, 2007, pp. 125–140.

[9]Slavinskaya, N. A., Riedel, U., Dworkin, S. B., and Thomson, M. J., "Detailed Numerical Modeling of PAH Formation and Growth in Non-premixed Ethylene and Ethane Flames," *Combustion and Flame*, Vol. 159, No. 3, 2012, pp. 979–995.

[10]Olm, C., Zsély, I. G., Varga, T., Curran, H. J., and Turányi, T., "Comparison of the Performance of Several Recent Syngas Combustion Mechanisms," *Combustion and Flame*, Vol. 162, No. 5, 2015, pp. 1793–1812.

[11]Atkinson, R., Baulch, D. L., Cox, R. A., Crowley, J. N., Hampson, R. F., Hynes, R. G., Jenkin, M. E., Rossi, M. J., and Troe, J., "Evaluated Kinetic and Photochemical Data for Atmospheric Chemistry: Volume I - Gas Phase Reactions of O_x, HO_x, NO_x and SO_x Species," *Atmospheric Chemistry and Physics,* Vol. 4, 2004, pp. 1461–1738.

[12]Wang, H., You, X., Joshi, A. V., Davis, S. G., Laskin, A., Egolfopoulos, F., and Law, C. K., "USC Mech Version II. High-Temperature Combustion Reaction Model of H_2/CO/C1-C4 Compounds," URL: http://ignis.usc.edu/USC_Mech_II.htm.

[13]Miller, J. A., and Melius, C. F., "Kinetic and Thermodynamic Issues in the Formation of Aromatic Compounds in Flames of Aliphatic Fuels," *Combustion and Flame*, Vol. 91, No. 1, 1992, pp. 21–39.

[14]Kathrotia, T., Fikri, M., Bozkurt, M., Hartmann, M., Riedel, U., and Schulz, C., "Study of the H+O+M Reaction Forming OH^*: Kinetics of OH^* Chemiluminescence in Hydrogen Combustion Systems," *Combustion and Flame*, Vol. 157, No. 7, 2010, pp. 1261–1273.

[15]Baulch, D. L., "Evaluated Kinetic Data for Combustion Modeling: Supplement II," *Journal of Physical and Chemical Reference Data*, Vol. 34, No. 3, 2005, p. 757.

[16]Troe, J., "Detailed modeling of the temperature and pressure dependence of the reaction $H+O_2$ (+M)→HO_2 (+M)," *Proceedings of the Combustion Institute,* Vol. 28, No. 2, 2000, pp. 1463–1469.

[17]Cohen, N., Westberg, K. R., "Chemical Kinetic Data Sheets for High-Temperature Chemical Reactions," *Journal of Physical and Chemical Reference Data*, Vol. 12, No. 3, 1983, pp. 531-590.

[18]Zsély, I. G., Zádor, J., and Turányi, T., "Uncertainty Analysis of Updated Hydrogen and Carbon Monoxide Oxidation Mechanisms," *Proceedings of the Combustion Institute,* Vol. 30, No. 1, 2005, pp. 1273–1281.

[19]Sun, H., Yang, S. I., Jomaas, G., and Law, C. K., "High-pressure Laminar Flame Speeds and Kinetic Modeling of Carbon Monoxide/Hydrogen Combustion," *Proceedings of the Combustion Institute*, Vol. 31, No. 1, 2007, pp. 439–446.

[20]Troe, J. "Predictive Possibilities of Unimolecular Rate Theory," *The Journal of Physical Chemistry*, Vol. 83, No. 1, 1979, pp. 114–126.

[21] Li, J., Zhao, Z., Kazakov, A., Chaos, M., Dryer, F. L., and Scire, J. J., "A Comprehensive Kinetic Mechanism for CO, CH_2O, and CH_3OH Combustion," *International Journal of Chemical Kinetics*, Vol. 39, No. 3, 2007, pp. 109–136.

[22] Davidson, D. F., and Hanson, R. K., "Interpreting Shock Tube Ignition Data," *WSSCI Fall 2003 Meeting*, University of California at Los Angeles, 2003.

[23] Petersen, E. L., and Hanson, R. K., "Nonideal Effects Behind Reflected Shock Waves in a High-pressure Shock Tube," *Shock Waves*, Vol. 10, No. 6, 2001, pp. 405–420.

[24] Petersen, E. L., Rickard, M. J. A., Crofton, M. W., Abbey, E. D., Traum, M. J., and Kalitan, D. M., "A Facility for Gas- and Condensed-phase Measurements Behind Shock Waves," *Measurement Science and Technology*, Vol. 16, No. 9, 2005, pp. 1716–1729.

[25] Petersen, E. L., and Hanson, R. K., "Measurement of Reflected-shock Bifurcation Over a Wide Range of Gas Composition and Pressure," *Shock Waves*, Vol. 15, No. 5, 2006, pp. 333–340.

[26] Dryer, F. L., and Chaos, M., "Ignition of Syngas/Air and Hydrogen/Air Mixtures at Low Temperatures and High Pressures: Experimental Data Interpretation and Kinetic Modeling Implications," *Combustion and Flame*, Vol. 152, 1-2, 2008, pp. 293–299.

[27] Davidson, D. F., and Hanson, R. K., "Recent Advances in Shock Tube/Laser Diagnostic Methods for Improved Chemical Kinetics Measurements," *Shock Waves*, Vol. 19, No. 4, 2009, pp. 271–283.

[28] Ihme, M., "On the Role of Turbulence and Compositional Fluctuations in Rapid Compression Machines: Autoignition of Syngas Mixtures," *Combustion and Flame*, Vol. 159, No. 4, 2012, pp. 1592–1604.

[29] Urzay, J., Kseib, N., Davidson, D. F., Iaccarino, G., and Hanson, R. K., "Uncertainty-quantification Analysis of the Effects of Residual Impurities on Hydrogen–oxygen Ignition in Shock Tubes," *Combustion and Flame*, Vol. 161, No. 1, 2014, pp. 1–15.

[30] Mansfield, A. B., and Wooldridge, M. S., "High-pressure Low-temperature Ignition Behavior of Syngas Mixtures," *Combustion and Flame*, Vol. 161, No. 9, 2014, pp. 2242–2251.

[31] Grogan, K. P., and Ihme, M., "Weak and Strong Ignition of Hydrogen/Oxygen Mixtures in Shock-tube Systems," *Proceedings of the Combustion Institute*, Vol. 35, No. 2, 2015, pp. 2181–2189.

[32] Kalitan, D. M., Mertens, J. D., Crofton, M. W., and Petersen, E. L., "Ignition and Oxidation of Lean CO/H2 Fuel Blends in Air," *Journal of Propulsion and Power*, Vol. 23, No. 6, 2007, pp. 1291–1301.

[33] Petersen, E. L., Kalitan, D. M., Barrett, A. B., Reehal, S. C., Mertens, J. D., Beerer, D. J., Hack, R. L., and McDonell, V. G., "New Syngas/Air Ignition Data at Lower Temperature and Elevated Pressure and Comparison to Current Kinetics Models," *Combustion and Flame*, Vol. 149, 1-2, 2007, pp. 244–247.

[34] Mertens, J. D., Kalitan, D. M., Barrett, A. B., and Petersen, E. L., "Determination of the Rate of $H+O_2+M \rightarrow HO_2+M$ (M=N_2, Ar, H_2O) from Ignition of Syngas at Practical Conditions," *Proceedings of the Combustion Institute*, Vol. 32, No. 1, 2009, pp. 295–303.

[35] Herzler, J., and Naumann, C., "Shock Tube Study of the Ignition of Lean CO/H_2 Fuel Blends at Intermediate Temperatures and High Pressure," *Combustion Science and Technology*, Vol. 180, 10-11, 2008, pp. 2015–2028.

[36] Kéromnès, A., Metcalfe, W. K., Heufer, K. A., Donohoe, N., Das, A. K., Sung, C.-J., Herzler, J., Naumann, C., Griebel, P., Mathieu, O., Krejci, M. C., Petersen, E. L., Pitz, W. J., and Curran, H. J., "An Experimental and Detailed Chemical Kinetic Modeling Study of Hydrogen and Syngas Mixture Oxidation at Elevated Pressures," *Combustion and Flame*, Vol. 160, No. 6, 2013, pp. 995–1011.

[37] Bouvet, N., Chauveau, C., Gökalp, I., and Halter, F., "Experimental Studies of the Fundamental Flame Speeds of Syngas (H_2/CO)/Air Mixtures," *Proceedings of the Combustion Institute*, Vol. 33, No. 1, 2011, pp. 913–920.

[38] Esposito, G., and Chelliah, H. K., "Effect of Binary Diffusion and Chemical Kinetic Parameter Uncertainties in Simulations of Premixed and Non-premixed Laminar Hydrogen Flames," *Combustion and Flame*, Vol. 159, 2012, pp. 3522–3529.

[39] Goswami, M., Derks, S. C., Coumans, K., Slikker, W. J., Andrade Oliveira, M. H. de, Bastiaans, R. J., Luijten, C. C., Goey, L. P. H. de, and Konnov, A. A., "The Effect of Elevated Pressures on the Laminar Burning Velocity of Methane+Air Mixtures," *Combustion and Flame*, Vol. 160, No. 9, 2013, pp. 1627–1635.

[40] Egolfopoulos, F. N., Hansen, N., Ju, Y., Kohse-Höinghaus, K., Law, C. K., and Qi, F., "Advances and Challenges in Laminar Flame Experiments and Implications for Combustion Chemistry," *Progress in Energy and Combustion Science*, Vol. 43, 2014, pp. 36–67.

[41] Krejci, M. C., Mathieu, O., Vissotski, A. J., Ravi, S., Sikes, T. G., Petersen, E. L., Kérmonès, A., Metcalfe, W., and Curran, H. J., "Laminar Flame Speed and Ignition Delay Time Data for the Kinetic Modeling of Hydrogen and Syngas Fuel Blends," *Journal of Engineering for Gas Turbines and Power*, Vol. 135, No. 2, 2013, p. 021503.

[42] Natarajan, J., Lieuwen, T., and Seitzman, J., "Laminar Flame Speeds of H_2/CO Mixtures: Effect of CO_2 Dilution, Preheat Temperature, and Pressure," *Combustion and Flame*, Vol. 151, 1-2, 2007, pp. 104–119.

[43] Hassan, M. I., Aung, K. T., and Faeth, G. M., "Properties of Laminar Premixed CO/H/Air Flames at Various Pressures," *Journal of Propulsion and Power*, Vol. 13, No. 2, 1997, pp. 239–245.

[44] Natarajan, J., Kochar, Y., Lieuwen, T., and Seitzman, J., "Pressure and Preheat Dependence of Laminar Flame Speeds of H_2/CO/CO_2/O_2/He Mixtures," *Proceedings of the Combustion Institute*, Vol. 32, No. 1, 2009, pp. 1261–1268.

[45] Kee, R. J., Rupley, F. M., and Miller, J. A., "CHEMKIN-II: A FORTRAN chemical kinetics package for the analysis of gas-phase chemical kinetics," SAND89-8009B, UC-706; Sandia National Laboratories: Albuquerque, NM, 1993.

[46] Kintech Lab Ltd., "Chemical Workbench®," Software Package, URL: http://www.kintechlab.com/.
[47] You, X., Russi, T., Packard, A., and Frenklach, M., "Optimization of Combustion Kinetic Models on a Feasible Set," *Proceedings of the Combustion Institute*, Vol. 33, No. 1, 2011, pp. 509–516.
[48] Mittal, G., Sung, C.-J., and Yetter, R. A., "Autoignition of H_2/CO at Elevated Pressures in a Rapid Compression Machine," *International Journal of Chemical Kinetics*, Vol. 38, No. 8, 2006, pp. 516–529.
[50] Karkach, S. P., Osherov, V. I., "*Ab Initio* Analysis of the Transition States on the Lowest Triplet H_2O_2 Potential Surface," *The Journal of Chemical Physics*, Vol. 110, 1999, pp. 11918–11927.